Seismic behavior factors of buckling-restrained braced frames

Jinkoo Kim[†] and Junhee Park

Department of Architectural Engineering, Sungkyunkwan University, Suwon, Korea

Sang-Dae Kim

School of Civil, Environmental and Architectural Engineering, Korea University, Seoul, Korea

Abstract.   The seismic behavior of a framed structure with chevron-type buckling restrained braces was investigated and their behavior factors, such as overstrength, ductility, and response modification factors, were evaluated. Two types of structures, building frame systems and dual systems, with 4, 8, 12, and 16 stories were designed per the IBC 2003, the AISC LRFD and the AISC Seismic Provisions. Nonlinear static pushover analyses using two different loading patterns and incremental dynamic analysis using 20 earthquake records were carried out to compute behavior factors. Time history analyses were also conducted with another 20 earthquakes to obtain dynamic responses. According to the analysis results, the response modification factors turned out to be larger than what is proposed in the provision in low-rise structures, and a little smaller than the code-values in the medium-rise structures. The dual systems, even though designed with smaller seismic load, showed superior static and dynamic performances.

Keywords: buckling restrained braces; behavior factors; response modification factors; seismic design; building systems.

1. Introduction

The buckling restrained braces (BRBs), which can yield under both tension and compression, have gained acceptance in many countries around the world. Clark *et al.* (1999) showed that for the same loading condition buckling-restrained braced frames (BRBF) could be designed with 50% of the steel weight of special moment resisting frames. According to the previous experimental research BRB behaves stably under cyclic loads, dissipating large amount of hysteretic energy (Black *et al.* 2002, Merrit *et al.* 2003). Iwata and Murai developed a buckling-restrained brace formed by welding a core plate covered with unbonded material to a pair of mortar-filled channel steels. Tremblay *et al.* (2006) performed subassemblage seismic tests on the conventional concrete-filled buckling-restrained braces and the BRB composed of steel core restrained by hollow steel sections, and found that the BRBs exhibited good performance under the quasi-static and dynamic

---

† Corresponding author, E-mail: jkim12@skku.edu

loading sequences. Kim *et al.* (2004) and Choi and Kim (2009) developed an energy-based seismic design procedure for buckling-restrained braces. Based on the satisfactory performance obtained from various experiments, BRBs have been actively applied to seismic design and retrofit of building structures in high seismic regions, such as Taiwan, Japan, and United States. It was reported that BRBs were used in almost 60% of high-rise steel buildings constructed recently in Japan (Xie 2005). Recently BRB's were also applied to seismic design and upgrading of steel bridges (Carden *et al.* 2006, Usami *et al.* 2005).

To accommodate the application of BRBs and to provide basic requirements for the seismic design of BRBFs, AISC (American Institute of Steel Construction) and SEAOC (Structural Engineers Association of California) proposed the Recommended Provision for Buckling-Restrained Braced Frames (2001). This was later adapted to the NEHRP Recommended Provisions for Seismic Regulations for New Buildings and Other Structures (FEMA-450) and to the AISC Seismic Provisions for Structural Steel Buildings (2005) with some modifications. One of the most significant changes was the reduction of response modification factors for BRBF: the AISC/SEAOC Recommended Provision proposed 8.0 and 9.0 for the response modification factor for buckling-restrained building frame systems and dual systems. They were reduced to 7.0 and 8.0 when they were adapted to the FEMA-450 and the AISC Seismic Provision.

The role of behavior factors, such as overstrength, ductility, and the response modification factors, is essential in designing the earthquake load-resisting elements. Among them, the response modification factor (or R-factor), which represents the ratio of the forces that would develop if the structure is to behave elastically to the prescribed design forces at the strength limit state, is used to reduce the seismic design force. Such a design concept is based on the assumption that well-detailed structures can develop lateral strength in excess of their design strength and sustain large inelastic deformation without collapse.

It was commented in documents such as ATC-19 (1995) and ATC-34 (1995) that the response modification factor can be calculated as the product of many behavior factors such as overstrength factors, ductility factors, damping factors, and redundancy factors. Osteraas and Krawinkler (1990) conducted a detailed study of reserve strength of concentric braced frames designed per Uniform Building Code seismic zone 4 and soil type S2. Balendra and Huang (2003) found that the response modification factors decreased when the number of stories increased. Maheri and Akbari (2003) investigated the response modification factors of steel-braced reinforced concrete framed dual systems. Kim and Choi (2005) investigated response modification factors of steel chevron braced frames. According to the results of above studies, the response modification factors of braced frames appear to be period and applied load-dependent contrary to seismic design codes prescribing values regardless of building height and earthquake load level.

In this study the nonlinear behavior of structures with BRBs was investigated and the validity of the code-specified response modification factors were verified. Two types of structures, building frame systems (BFS) and dual systems (DS), with 4, 8, 12, and 16 stories were designed. Nonlinear static pushover analyses were carried out to identify the load-displacement relationship and the behavior factors. For comparison with static analysis results, the incremental dynamic analyses were also conducted to obtain the behavior factors, which were compared with the values obtained by pushover analysis and those presented in the design provisions. Time history analyses were also carried out to observe the dynamic behaviors.

2. Design of analysis models

To observe nonlinear behavior and to evaluate the behavior factors of BRBFs, 4, 8, 12, and 16 story three-bay structures with the span length of 12 m and the story height of 3.6 m were designed per the US 2003 IBC (2003) and the AISC Load and Resistance Factor Design (1998). The Seismic Provisions for Structural Steel Buildings (2005) was also used in the structural design. Fig. 1(a) shows the structural plan of the prototype structure, where the chevron-type BRBs are located in the mid-bay of the perimeter frames (Fig. 1(b)). The perimeter braced frame marked in Fig. 1(a) was analyzed using the program code Drain 2DX (Prakash *et al.* 1993). The braced frames with BRBs were designed as: (1) building frame systems with pin-connected beam-column joints; and (2) dual systems with the moment frames resisting 25% of the lateral load. The following loads were considered in the structural design: dead and live loads of 4.90 kN/m^2 and 2.45 kN/m^2, respectively; and the earthquake loads determined based on the 2003 International Building Code (Seismic Use Group II, soil type D). The response modification factors of 7 and 8 were used in the design of the building frame systems and the dual systems with BRBs, respectively, as suggested in the Seismic Provisions for Structural Steel Buildings. Table 1 shows the design coefficients recommended in the Seismic Provisions. All the columns and beams were made of SM490 ($F_y = 32.37$ kN/cm^2) and SS400 ($F_y = 23.54$ kN/cm^2), respectively, and the core of a BRB is made of SS400. To take the conventional design practice into consideration, the same structural members were used in two consecutive stories except for the 4-story structures; the ratio of the member force induced by the applied loads to nominal strength of the structural members is maintained to be 0.98 to 0.99. The selected structural members of the model structures are listed in Table 2. The natural periods and
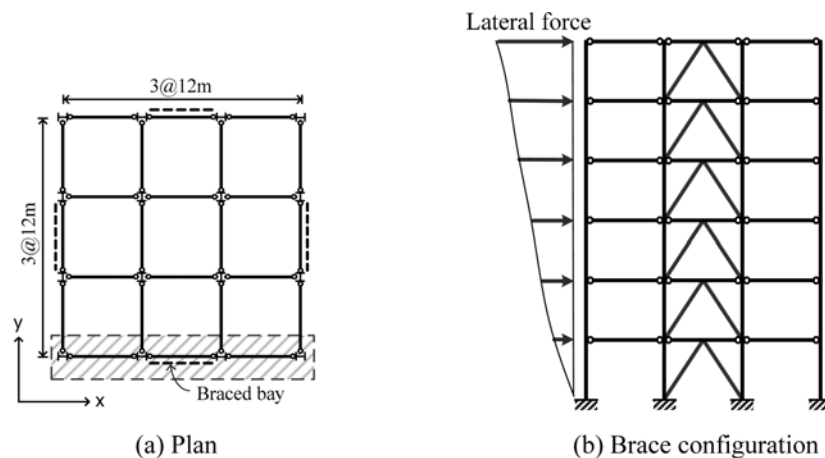

(a) Plan   (b) Brace configuration

Fig. 1 Configuration of the model structures

Table 1 Behavior factors of BRBF (Non-moment-resisting connections)

	Response modification factors	Overstrength factors	Deflection amplification factors
Building Frame Systems (BFS)	7	2	5.5
Dual Systems (DS)	8	2.5	5

Table 2 Size of structural members (unit: mm)

(a) 4-story structures

	story	BFS	DS
Exterior columns	1	H 298×299×9×14	H 350×357×19×19
	4	H 150×150×7×10	H 300×300×10×15
Exterior beams	1	H 692×300×12×17	H 692×300×20×12
	4	H 692×300×12×17	H 692×300×20×12
Braces	1	H 310×310×15×20	H 310×300×15×20
	4	H 290×285×12×12	H 290×285×12×12

(b) 8-story structures

	story	BFS	DS
Exterior columns	1~2	H 394×405×18×18	H 414×405×18×28
	7~8	H 200×200× 8×12	H 300×305×15×15
Exterior beams	1~2	H 692×300×12×17	H 900×300×20×32
	7~8	H 692×300×12×17	H 800×300×14×26
Braces	1~2	H 400×400×18×21	H 344×348×10×16
	7~8	H 338×351×13×13	H 250×250× 9×14

(c) 12-story structures

	story	BFS	DS
Exterior columns	1~2	H 428×407×20×35	H 500×500×30×50
	7~8	H 200×200× 8×12	H 344×354×16×16
Exterior beams	1~2	H 692×300×12×17	H 912×302×18×34
	7~8	H 692×300×12×17	H 708×302×15×28
Braces	1~2	H 390×390×15×28	H 350×350×12×19
	7~8	H 340×330×13×13	H 244×252×11×11

(d) 16-story structures

	story	BFS	DS
Exterior columns	1~2	H 410×410×30×40	H 500×500×30×50
	7~8	H 200×200× 8×12	H 350×350×12×19
Exterior beams	1~2	H 692×300×12×17	H 912×302×30×40
	7~8	H 692×300×12×17	H 708×302×15×28
Braces	1~2	H 400×400×18×28	H 344×354×16×16
	7~8	H 300×300×10×15	H 244×252×11×11

Table 3 Modal participation factors of the model structures

Structure	Mode	Period (sec)		Modal participation factors (%)	
		BFS	DS	BFS	DS
4-story	1	0.44	0.52	82.02	83.07
	2	0.17	0.20	13.57	12.83
	3	0.10	0.12	3.23	2.73
8-story	1	0.80	0.87	73.59	77.47
	2	0.28	0.31	17.69	14.64
	3	0.15	0.17	4.57	3.94
12-story	1	1.23	1.42	69.45	70.85
	2	0.41	0.48	19.42	17.90
	3	0.22	0.26	5.27	5.39
16-story	1	1.72	1.95	66.78	70.23
	2	0.55	0.62	19.86	18.34
	3	0.29	0.33	5.79	5.04
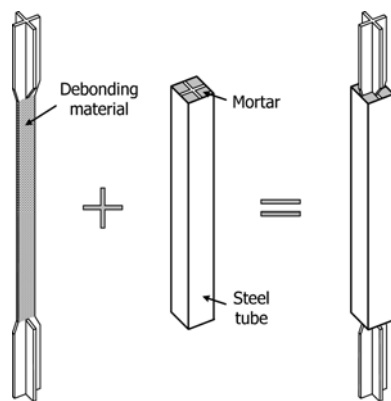
Fig. 2 Configuration of a typical buckling-restrained brace
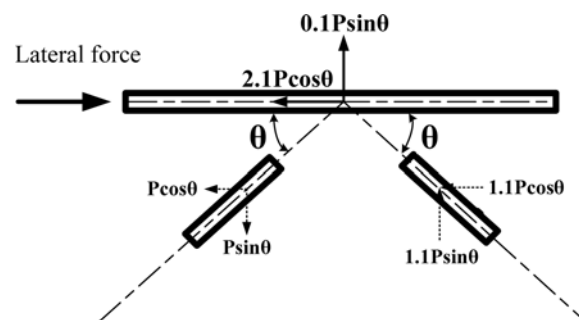
Fig. 3 Unbalanced force acting on the girder in the braced bay

the modal participation factors are presented in Table 3, in which it can be noticed that the modal participation of the fundamental mode of the dual systems is larger than that of the building frame systems.

In this study the typical buckling-restrained braces made of a steel core enclosed by a steel tube filled with mortar (Fig. 2) were used as bracing members in the analysis model structures. According to the test results of Black *et al*. (2002) and Merritt *et al*. (2003), the compressive yield stress of such a typical BRB is 3 to 10% higher than tensile yield stress due to the confining effect of the mortar and the external tube. In consideration of this observation, the compressive yield stress of BRB was taken to be 10% higher than the tensile yield stress in the analysis. This leads to the upward unbalanced force acting in the middle of the braced-bay girders as shown in Fig. 3.

3. Nonlinear behavior of the model structures

The relationship between the base shear and the top story displacement, which is generally called pushover curve or capacity curve, can be obtained by gradually increasing the lateral load appropriately distributed over the stories. There can be many alternatives for the distribution pattern of the lateral loads, and it may be expected that different patterns of lateral loads result in pushover curves with different characteristics and different sequence of plastic hinge formation. In this study the pushover curves were obtained by applying two different patterns of lateral seismic loads; forces are applied in proportion to:

(i) the product of story masses and the fundamental mode shape of the elastic model structure

$$F_i = \frac{m_i \phi_{i1}}{\displaystyle\sum_{i=1}^{N} m_i \phi_{i1}} V \tag{1}$$

where F_i is the seismic story force in the ith floor, m_i is the mass of the ith floor, ϕ_{i1} is the ith component of the mode shape vector for the fundamental mode, V is the base shear, and N is the number of floors.

(ii) the equivalent mode shape considering higher modes (Valles *et al.* 1996)

$$F_i = \frac{m_i \bar{\phi}_i}{\displaystyle\sum_{i=1}^{N} m_i \bar{\phi}_i} V \tag{2}$$

where $\bar{\phi}_i = \sqrt{\displaystyle\sum_{i=1}^{N} (\phi_{ij}\Gamma_j)^2}$ and $\Gamma_j = \dfrac{\displaystyle\sum_{i=1}^{N} m_i \phi_{ij}}{\displaystyle\sum_{i=1}^{N} m_i \phi_{ij}^2}$

Eigenvalue analyses were conducted first to determine the elastic natural periods and mode shapes of the model structures. Fig. 4 shows the shapes of the first mode and the equivalent mode of the 8-story model structures. Nonlinear static pushover analyses were carried out to evaluate the global yield limit state and the structural capacity by progressively increasing the lateral story forces proportional to the fundamental and the equivalent modes. The post-yield stiffness of the beams and columns was assumed to be 2% of the initial stiffness, and that of the braces was assumed to be zero. The expected yield stress of structural members was assumed to be 1.3 and 1.5 times the nominal yield stress for SM490 ($F_y = 323.7 \text{ N/mm}^2$) and SS400 ($F_y = 235.4 \text{ N/mm}^2$) steel, respectively.

For comparison with the results of the static pushover analysis, a series of incremental dynamic analyses (IDA) developed by Vamvatsikos and Cornell (2001) were performed to obtain load-displacement relationship of the model structures using the program DRAIN-2DX. The program implements a mixed implicit-explicit operator splitting method for dynamic analysis. The unconditionally stable Newmark method was employed for the integration associated with the linear responses and the explicit predictor-corrector method was applied for the integration of the nonlinear parts. Among the time history records developed for the SAC project (Somerville *et al.*
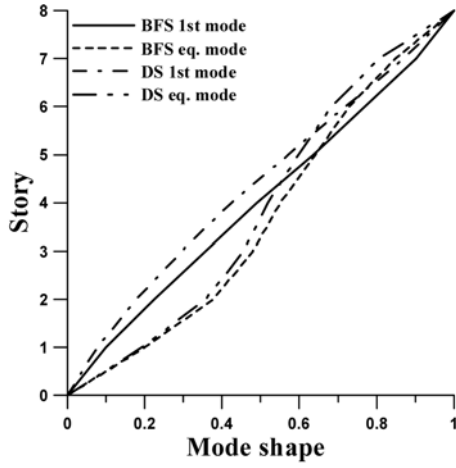
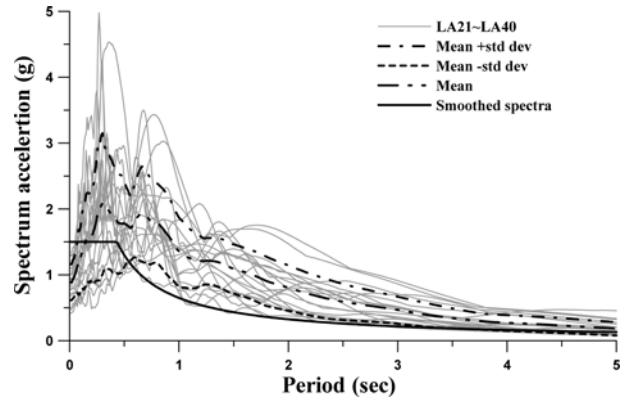Fig. 4 Mode shapes of the 8-story structures used in the pushover analysis

Fig. 5 Response spectra of the 20 earthquake records used for incremental dynamic analysis

(a) 4-story structure

(b) 8-story structure

(c) 12-story structure
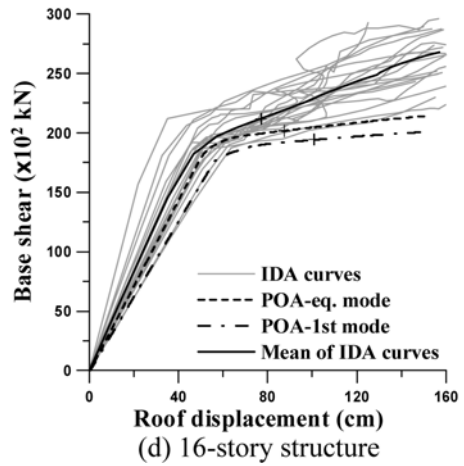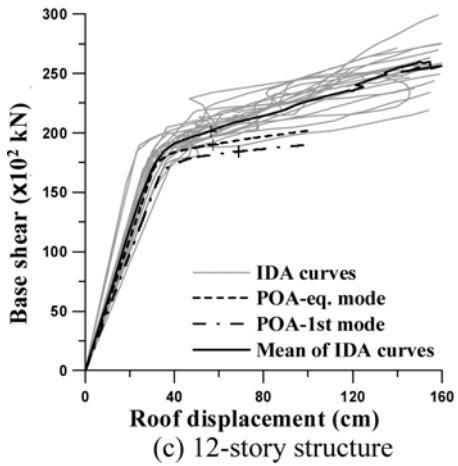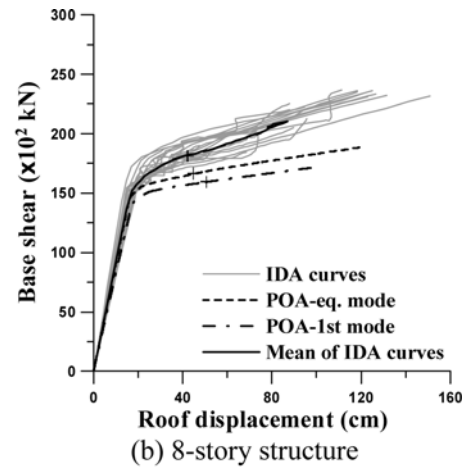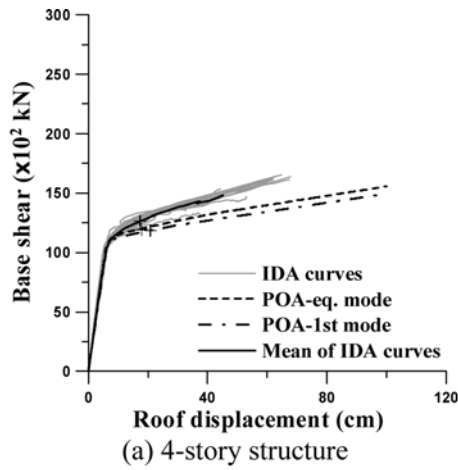

(d) 16-story structure

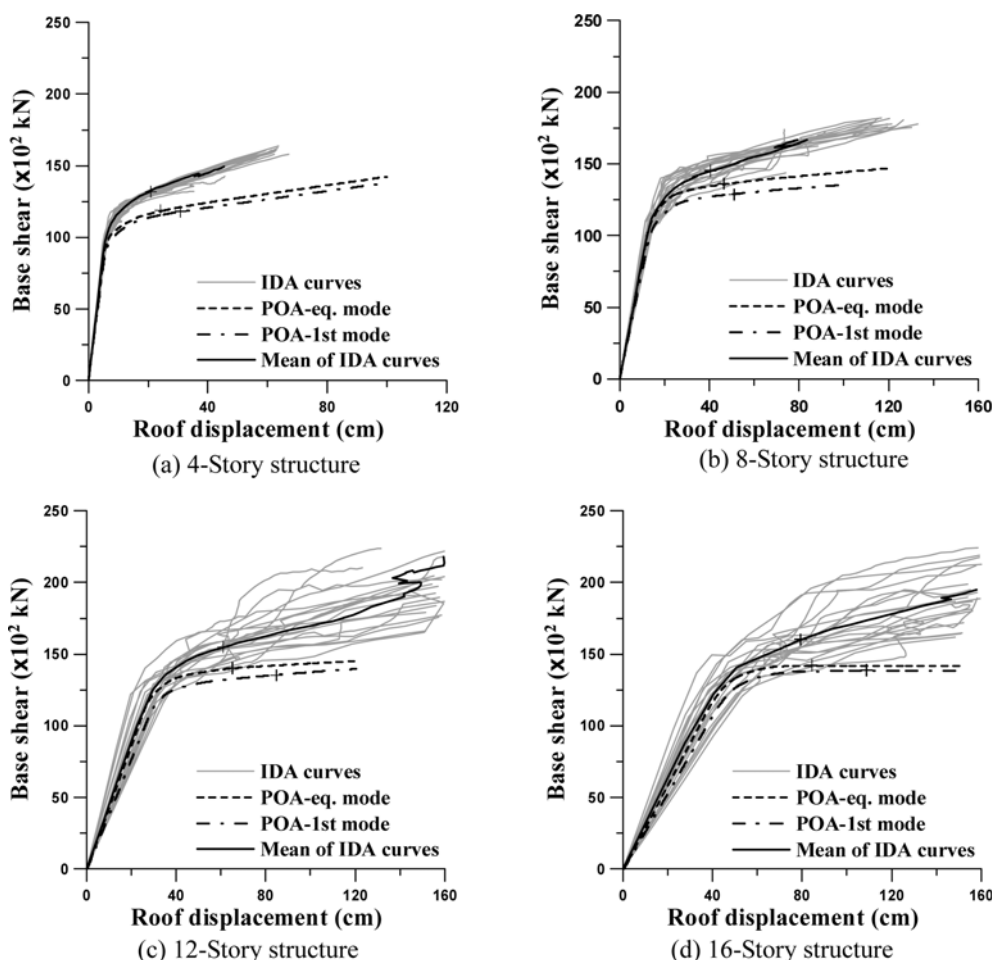Fig. 6 Pushover curves of the BFS model structures (+: 2.5% inter-story drift ratio)

Fig. 7 Pushover curves of the DS model structures (+: 2.5% inter-story drift ratio)

1997), 20 records with the 2% probability in 50 years (LA21~LA40) were selected for IDA. Fig. 5 plots the response spectra of the 20 earthquake records used for IDA. The dynamic pushover envelopes were obtained by plotting the point corresponding to the maximum base shear and the maximum top-story displacement computed for each scaled record. The amplitude of the accelerogram was increased by multiplying the accelerogram by a constant that increases the spectral ordinates of the accelerogram by 0.1 g. Figs. 6 and 7 show the load-displacement relationships of the model structures obtained from the static pushover analysis and the IDA. It can be observed that the results of the IDA generally form the upper bound of the pushover curves, and that when equivalent mode was used the stiffness and strength were slightly higher than those obtained using the first mode. It also can be noticed that the strengths of the building frame systems are higher than those of the dual systems designed with higher response modification factor, and that at the same ductility demand the dual systems show larger lateral displacements.

The limit state of a structure is defined by both the system-level criterion (maximum inter-story drift ratio) and the member-level criteria (limit states for BRB or columns). In the FEMA-356 (BSSC, 2000) the maximum inter-story drift ratio of 2.5% is generally specified as the collapse

prevention (CP) limit state for framed structures. In member level, the maximum ductility ratio of a brace under tension is given as 9 for collapse prevention stage. According to the experiments carried out by Black *et al.* (2002), however, the BRB remained stable until the ductility ratio reached 15. FEMA-356 also regulates the collapse prevention limit state of columns as follows

$$\theta_{CP} = 8\theta_y (P_{cr} < 0.2)$$

$$\theta_{CP} = 11\left(1 - 1.7\frac{P}{P_{cr}}\right)\theta_y\left(0.2 < \frac{P}{P_{cr}} < 0.5\right) \tag{3}$$

where P is the axial load acting on the column, P_{cr} is the compressive strength of the column, and θ_y is the rotation of the column at yield obtained as follows

$$\theta_y = \frac{ZF_{ye}l_c}{6EI_c}\left(1 - \frac{P}{P_{ye}}\right) \tag{4}$$

where Z is the plastic section modulus, F_{ye} is the expected yield strength, l_c is the length of the
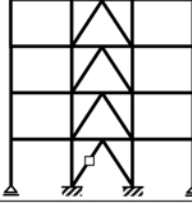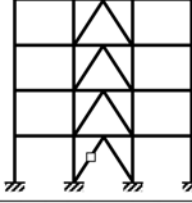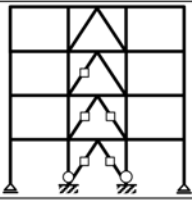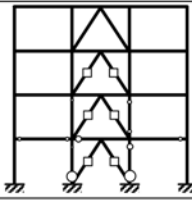
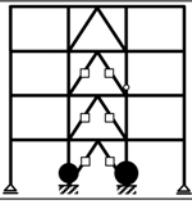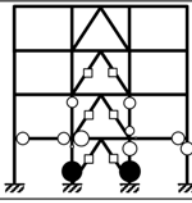|	BFS	DS
At first yield	□ Brace yield	□ Brace yield
Max. inter-story drift ratio(%)	0.4575 (at 3rd story)	0.4317 (at 1st story)
At brace ductility Demand=9 ($\mu_b = 9$)	○ Below CP stage □ Brace yield ○ 0.02 radian	○ Below CP stage □ Brace yield ○ 0.02 radian
Max. inter-story drift ratio(%)	3.1398 (at 1st story)	3.1738 (at 3rd story)
At brace ductility Demand=15 ($\mu_b = 15$)	○ Below CP stage ● Over CP stage □ Brace yield ○ 0.02 radian	○ Below CP stage ● Over CP stage □ Brace yield ○ 0.02 radian
Max. inter-story drift ratio(%)	5.4141 (at 1st story)	7.7863 (at 1st story)

Fig. 8 Plastic hinge formation in the 4-story structures at various state of brace ductility

column, E is the elastic modulus, l_c is the moment of inertia of the column, P is the column axial force at the target displacement, and P_{ye} is the expected yield force of the column. Therefore the plastic hinge rotation of a column depends on the factors such as material property and member force.

The location and magnitude of plastic hinges at each stage are plotted in Fig. 8, along with the maximum inter-story drift ratios. The results were obtained by pushover analysis using the lateral load pattern proportional to the fundamental mode shape. It can be noticed in the figure that at the maximum BRB ductility ratio of 9, the columns did not reach the limit state yet; however at the ductility ratio of 15, plastic rotation far exceeding the CP stage occurred at the first story columns. It also can be observed that large plastic hinges form at the bottom of the first story columns when the braces resist all lateral load (i.e., building frame systems), whereas small plastic hinges are
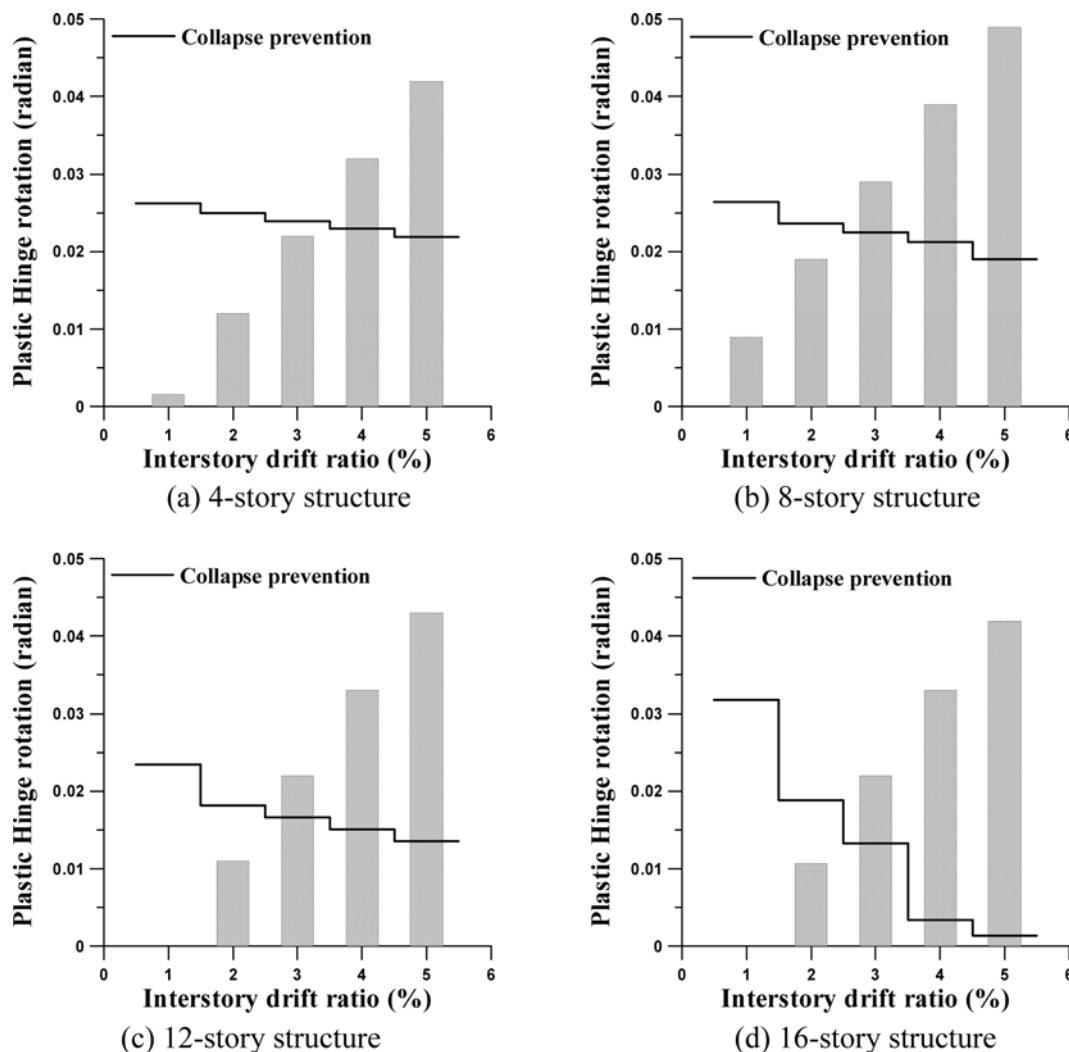

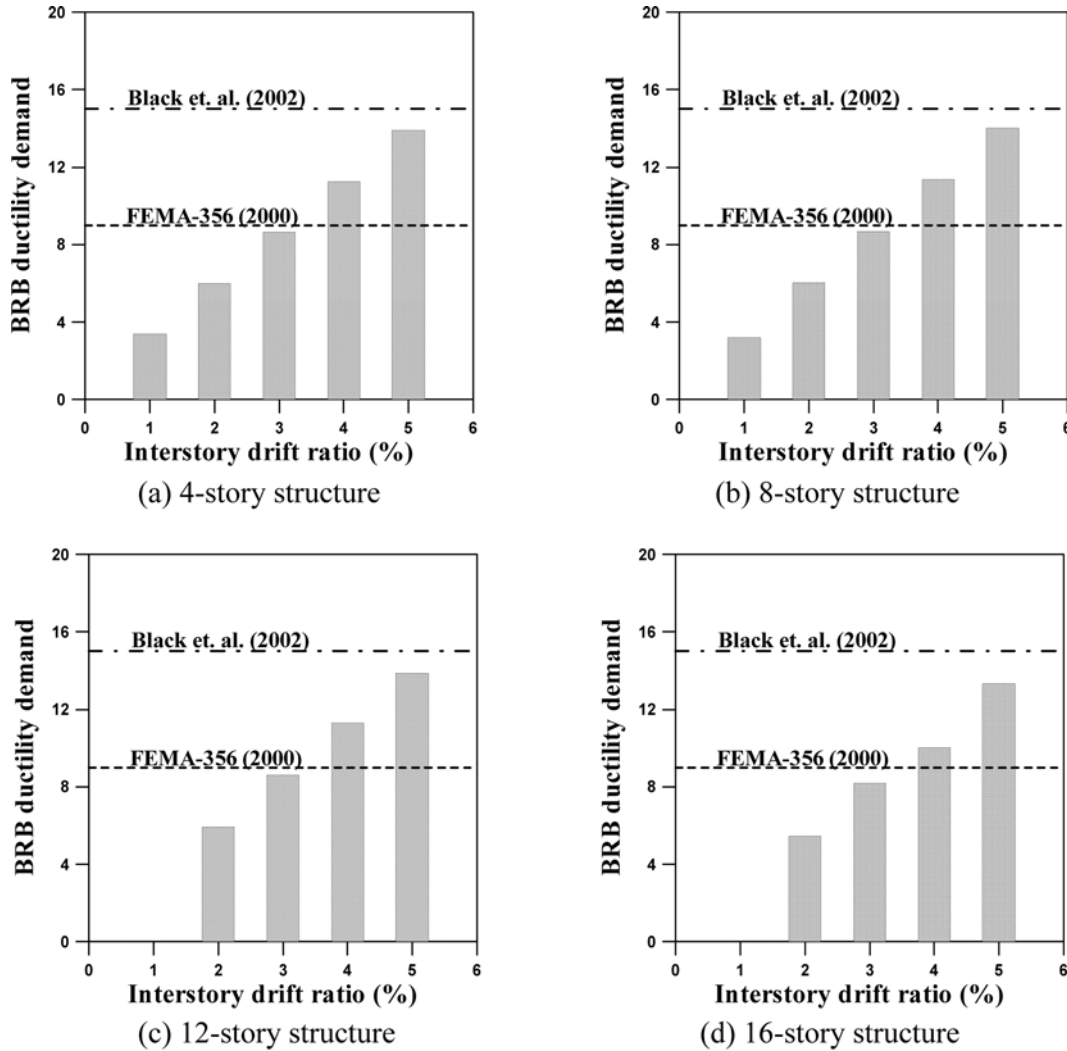Fig. 9 Plastic hinge rotation of columns at various maximum inter-story drifts

Fig. 10 Ductility demand of BRB at various maximum inter-story drifts

distributed to other columns and girders when part of the lateral load is shared by the moment frames (dual systems).

Fig. 9 shows the maximum plastic hinge rotation of columns in the model structures at various maximum inter-story drift ratios. The collapse prevention limit state computed by Eq. (3) is also plotted. It can be observed that the maximum plastic hinge rotations in columns of the 4-story structures reached those values regulated in the FEMA-356 when the maximum inter-story drift ratio reached about 3%. In the higher structures, the maximum plastic hinge rotation generally reached the limit state when the inter-story drift was about 2.5% of the story height. Fig. 10 depicts the maximum ductility demand of BRBs at various maximum inter-story drift ratios, where it can be observed that the limit state for collapse prevention performance criterion (which is 9) was reached when the maximum inter-story drift ratio became larger than 3%.
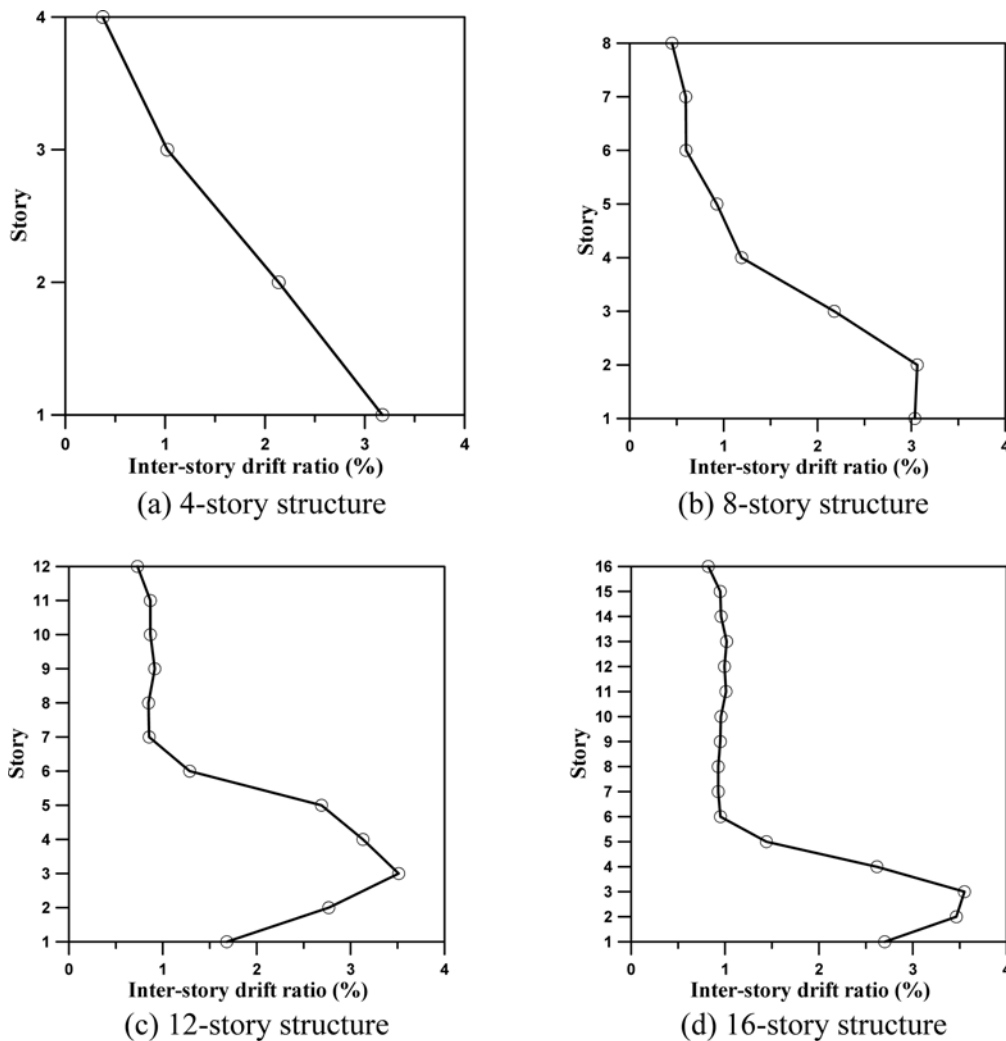
Fig. 11 Inter-story drifts of the model structures when the maximum BRB ductility ratio reaches 9.0

Fig. 11 shows the inter-story drifts of the model structures when the ductility demand of BRB reached 9.0. It can be observed that as the height of the structure increases large inter-story drift occurs localized in the lower part of the structure. Current study shows that at the CP stage of BRB, the maximum inter-story drifts of all the model structures exceeded 2.5% of the story height.

Fig. 12 presents the story shear of the 4~16-story dual system structures subjected to the design seismic load. It can be observed that differently from the building frame systems, in which most of the lateral load is resisted by the braces, the rigid frames shares 10 to 30% of the story shear in the dual systems.
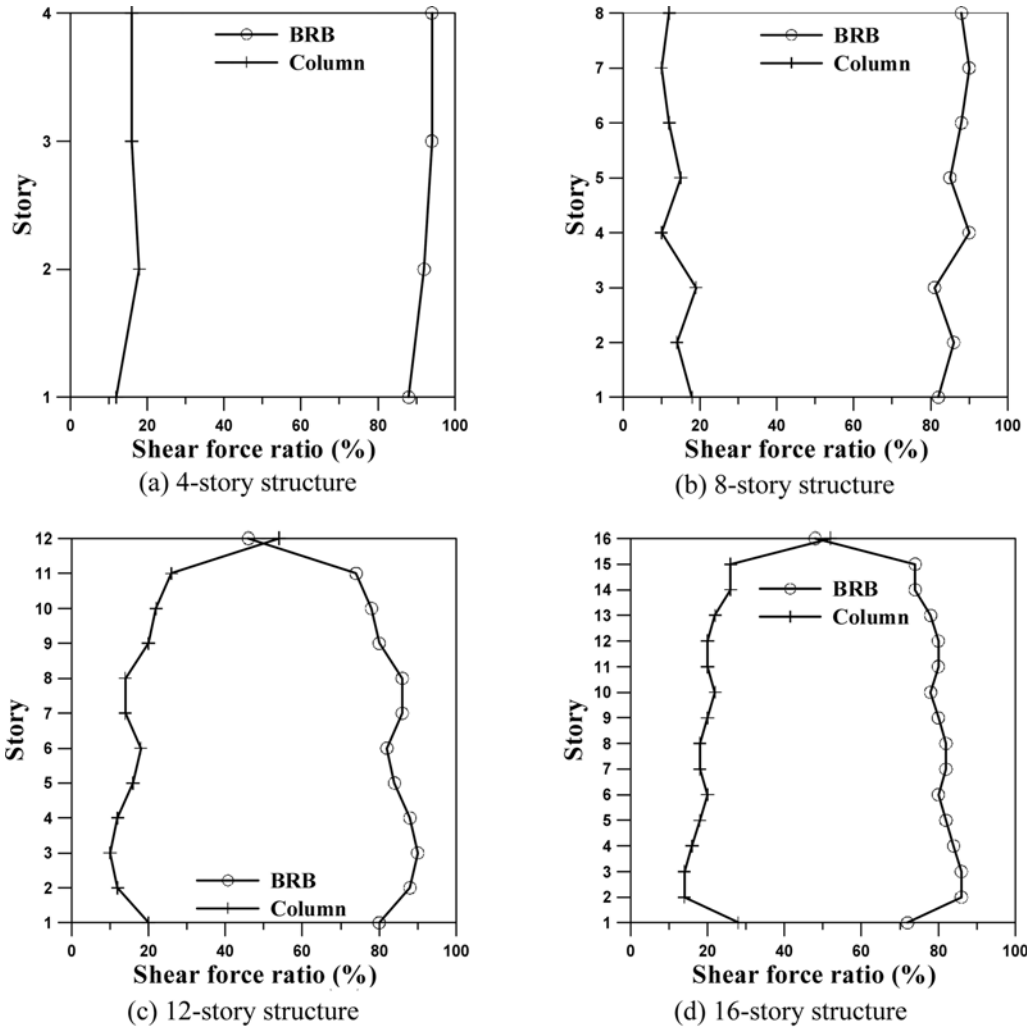
Fig. 12 Story shear distribution in dual systems

4. Computation of behavior factors

The ATC-19 (1995) proposed simplified procedure to estimate the response modification factors, in which the response modification factor, R-factor, is calculated as the product of the three parameters that profoundly influence the seismic response of structures

$$R = R_o R_\mu R_\gamma \tag{5}$$

where R_o is the overstrength factor to account for the observation that the maximum lateral strength of a structure generally exceeds its design strength. The FEMA-369 (BSSC 2001) specified three components of overstrength factors in Table C5.2.7-1: design overstrength, material overstrength, and system overstrength. R_μ is a ductility factor which is a measure of the global nonlinear response of a structure, and R_γ is a redundancy factor to quantify the improved reliability of seismic framing

systems constructed with multiple lines of strength. In this study the redundancy factor is assumed to be 1.0, and then the response modification factor is determined as the product of the overstrength factor and the ductility factor. Fig. 13 represents the typical base-shear versus roof displacement relation of a structure, which can be developed by a nonlinear static pushover analysis. From the figure, the overstrength factor and the ductility factor are defined as follows (ATC 1995)

$$R_o = \frac{V_y}{V_d}; \quad R_\mu = \frac{V_e}{V_y} \tag{6a,b}$$

where V_d is the design base shear, V_e is the maximum seismic demand for elastic response, and V_y is the base shear corresponding to the maximum inelastic displacement. The capacity envelopes can be utilized to evaluate overstrength factors. To find out the yield point, a straight line is drawn in such a way that the area under the original curve is equal to that of the idealized one. The base shear at yield and the maximum strength of all the analysis model structures obtained from the pushover analysis using the first mode loading pattern are presented in Table 4. The ductility factor is obtained using the system ductility factor by the procedure proposed by Newmark and Hall (1982)

$$R_\mu = 1.0 \qquad (T < 0.003\,\text{sec})$$

$$R_\mu = \sqrt{2\mu - 1} \quad (0.12 < T < 0.5\,\text{sec}) \tag{7}$$

$$R_\mu = \mu \qquad (T > 1.0\,\text{sec})$$

where T is the fundamental natural period of the structure, and μ is the ductility factor which is the maximum displacement divided by yield stress.
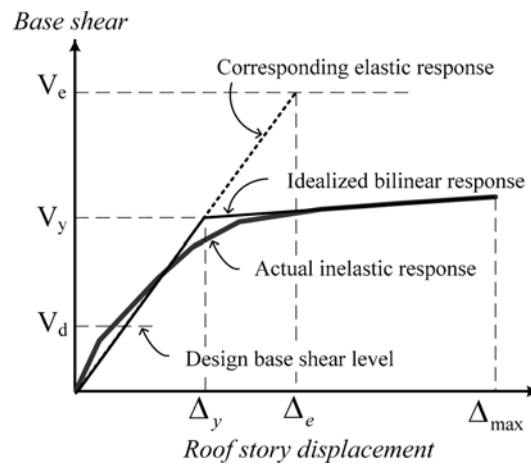

Fig. 13 Idealized base shear-roof story displacement relationship of a structure

Table 4 Results of pushover analyses using the first mode (unit: kN, cm)

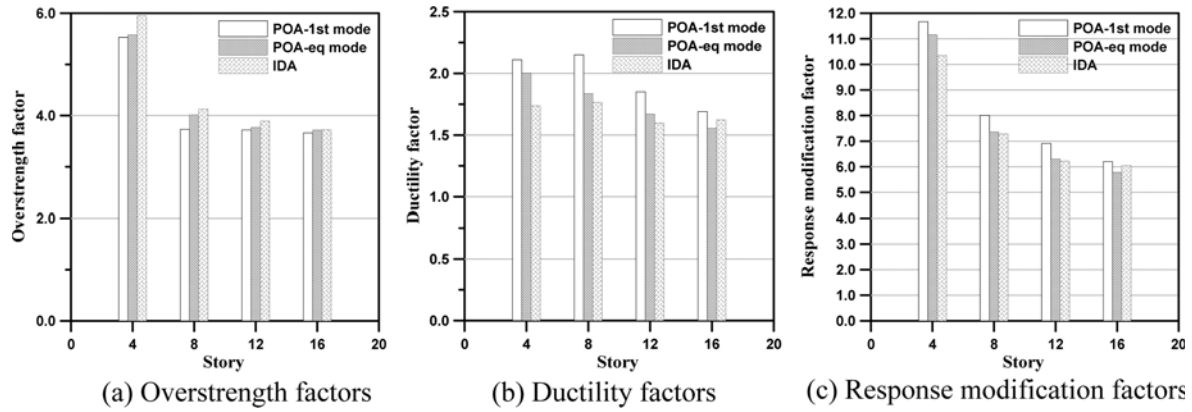| Model	4-story	8-story	12-story	16-story
V_d	1986.5	3973.0	4714.9	5066.5
V_y	11083.0	15938.0	17786.3	18843.7
Δ_y	8.2	19.2	34.7	56.3
Δ_{max}	20.4	37.0	57.9	87.5

Fig. 14 Behavior factors of the BFS model structures obtained from pushover analysis (POA) and incremental dynamic analysis (IDA)
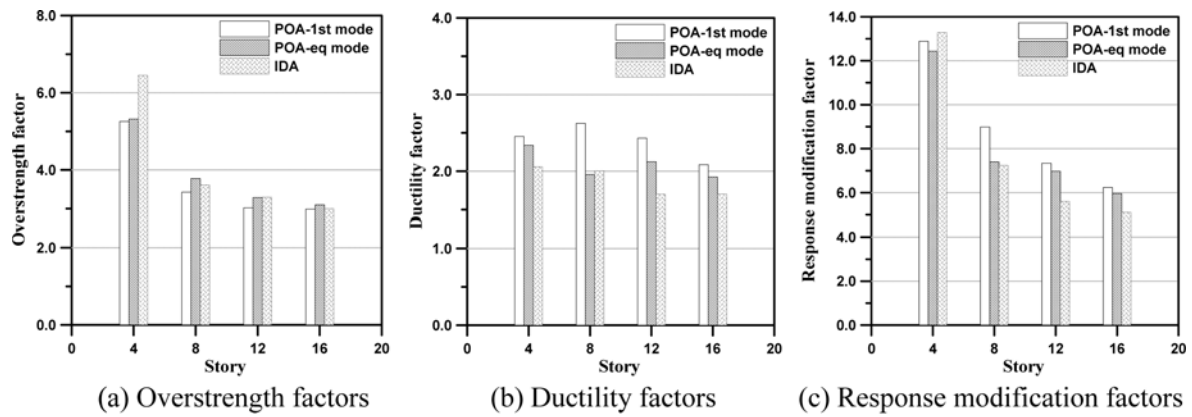

Fig. 15 Behavior factors of the DS model structures obtained from pushover analysis (POA) and incremental dynamic analysis (IDA)

The overstrength factors of the model structures were computed by Eq. (6a) based on the capacity envelops presented in Fig. 6 and Fig. 7 and are plotted in Figs. 14(a) and 15(a). For the incremental dynamic analysis results, the mean curves were used to derive the behavior factors. It can be seen that in every model structure the overstrength factor exceeds the value specified in the provision. It also can be observed that as the number of story increases the overstrength factors decrease rapidly. The dual systems, which were designed with larger response modification factor and therefore with smaller base shear, turned out to have smaller overstrength factors than those of the building frame systems. The overstrength factors obtained from the mean IDA curves were generally slightly larger than those obtained by static pushover analyses with two load patterns.

Figs. 14(b) and 15(b) plots the ductility factors of the model structures. It can be found that the ductility factor decreases as the number of story increases. It also can be seen that the ductility factors of dual systems are generally larger than those of building frame systems. The ductility factors obtained from the mean IDA curves were generally smaller than those from the pushover analyses.

The response modification factors are presented in Figs. 14(c) and 15(c), which are computed by multiplying the overstrength and the ductility factors using Eq. (5). It can be observed that the

response modification factor decreases as the number of story increases, which conforms to the results of the previous researches mentioned in the introduction. In the 4-story structures, the computed response modification factors turned out to be larger than 7.0 and 8.0 recommended in the seismic code for the building frame systems and the dual systems, respectively; however in the taller structures the factors became less than the code values. The computed response modification factors of the dual systems, which were designed with larger response modification factors and

Table 5 Response modification factors used in the design of the model structures

	System	4-story	8-Story	12-Story	16-Story
R-factor (Original)	BFS	8.0	8.0	8.0	8.0
	DS	9.0	9.0	9.0	9.0
R-factor (Redesigned)	BFS	11.0	7.5	6.0	5.5
	DS	12.5	7.5	7.0	6.0

(a) 4-story structures

(b) 8-story structures

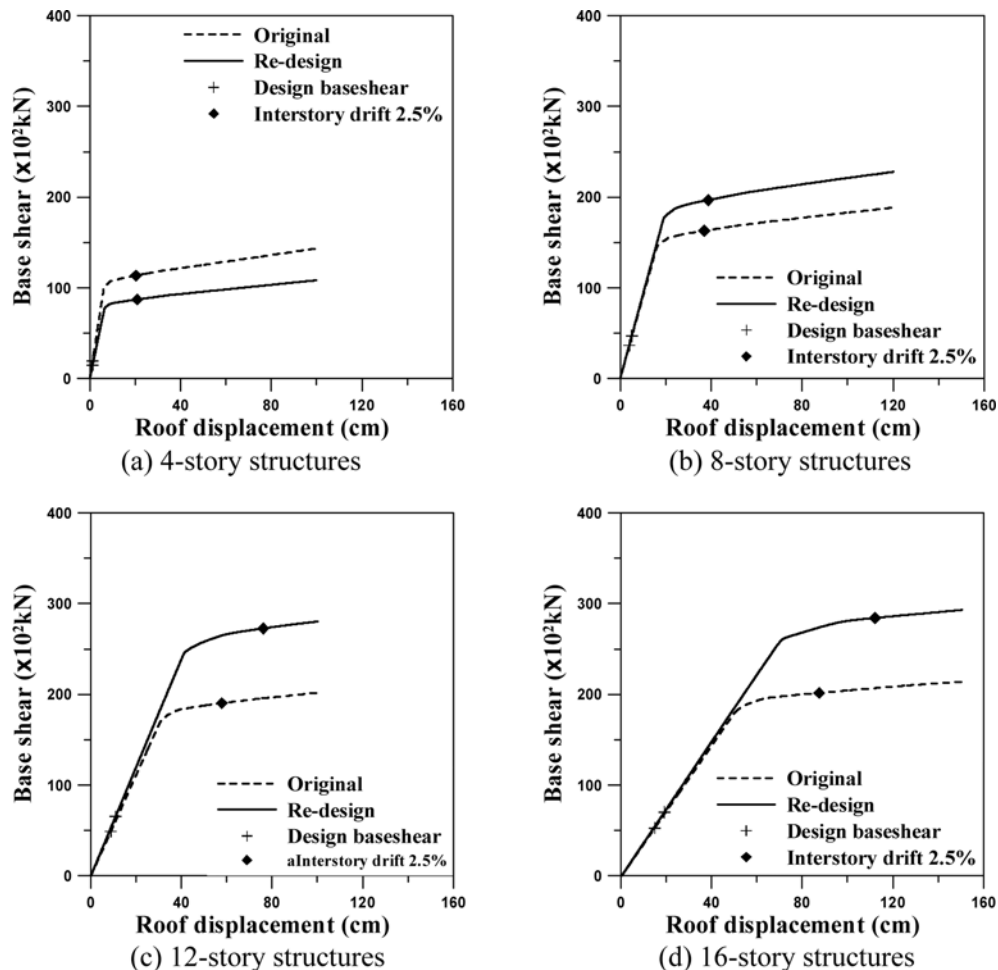(c) 12-story structures

(d) 16-story structures

Fig. 16 Pushover curves of the model structures re-designed using the newly-obtained response modification factors (building frame systems)

consequently with smaller design base shear, turned out to be generally larger than those of the building frame systems. The *R*-factors obtained using the mode shape of the fundamental mode turned out to be larger than those obtained using the equivalent mode shape. In most cases the *R*-factors obtained from the mean IDA curves were smaller than those computed from the pushover analyses. Table 5 shows the response modification factors computed from the pushover analyses with loading pattern proportional to the equivalent modes.

By using the response modification factors computed, the structures were redesigned and the previous procedures were followed again to reestimate the response modification factors. Figs. 16 and 17 present the pushover curves of the model structures designed using the code-specified *R*-factors and the structures redesigned using the computed response modification factors shown in Table 5. The dotted and the solid curves represent the pushover curves of the original and the redesigned structures, respectively. The strength of the redesigned 4-story structure, which used the increased *R*-factor, turned out to be smaller than that of the initial design. However the opposite was
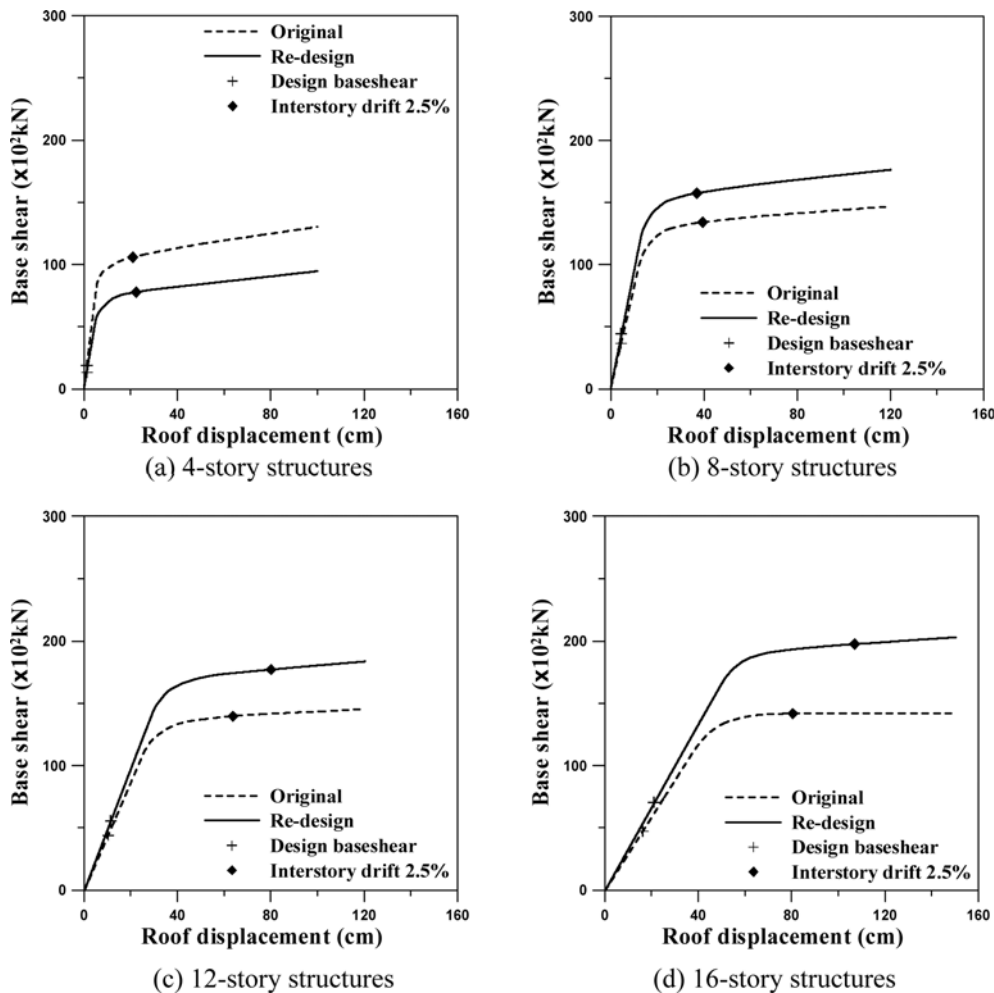

Fig. 17 Pushover curves of the model structures re-designed using the newly-obtained response modification factors (dual systems)
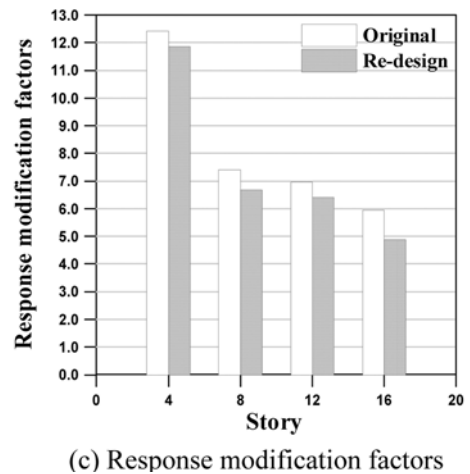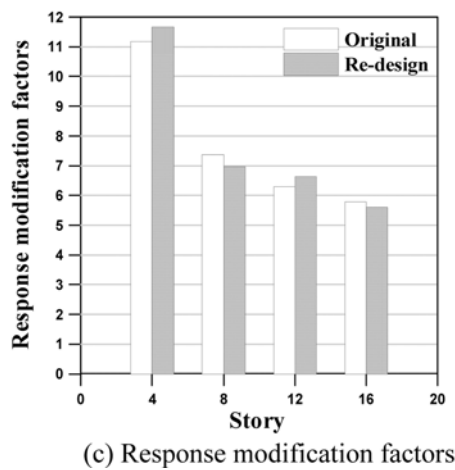
(a) Overstrength factors

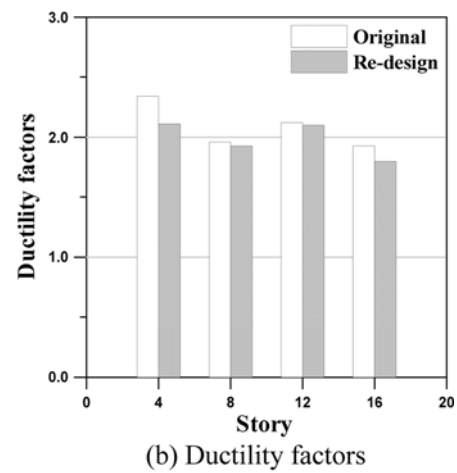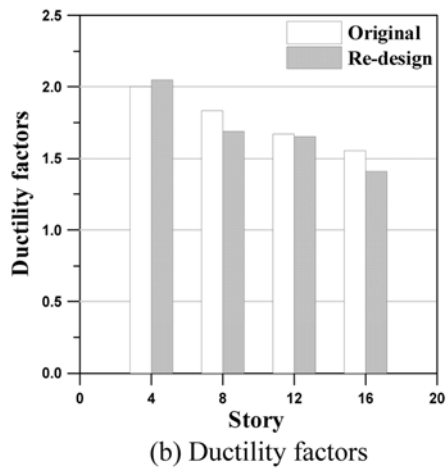

(b) Ductility factors

(c) Response modification factors
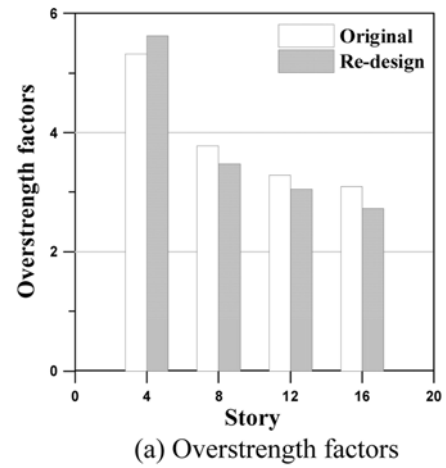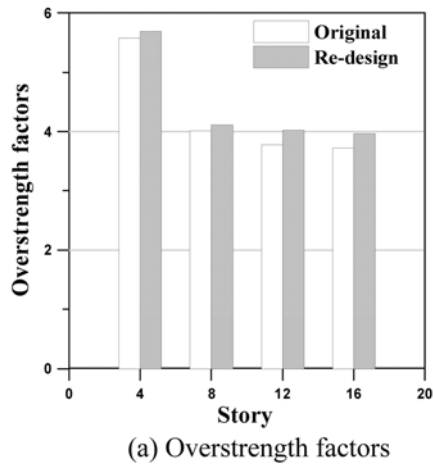
Fig. 18 Behavior factors of the original and the re-designed structures (building frame systems)

(a) Overstrength factors

(b) Ductility factors

(c) Response modification factors

Fig. 19 Behavior factors of the original and the re-designed structures (dual systems)

true in the taller structures which were redesigned using the decreased *R*-factors. Figs. 18 and 19 show the behavior factors of the original and the redesigned structures, where it can be noticed that the overstrength factors of the redesigned structures are slightly larger than those of the original structures and the ductility factors are generally slightly smaller than those of the original structures. This leaded to larger *R*-factors in the 4- and 12-story redesigned structures and to smaller *R*-factors in the 8- and 16-story redesigned structures. However the differences were not significant. Therefore, at least based on the limited analysis results of this study, it can be concluded that the behavior factors are not very sensitive to the design response modification factors. However it should be pointed out that the current response modification factors specified in the design code are generally overestimated, especially in the mid- to high-rise structures.

5. Dynamic analyses

Time-history analyses were conducted using the DRAIN-2DX to evaluate dynamic response of BRBFs. An ensemble of 20 earthquake records (LA01 − LA20) developed for the SAC Steel Project (1997) was used for dynamic analysis after scaled to fit the design spectrum corresponding to very rare event (2% probability of occurrence in 50 years) in Korea. The response spectra of the input records are compared with the design spectrum in Fig. 20. Fig. 21 presents the mean and the mean+standard deviation of the inter-story drifts of the 4- and the 12-story model structures obtained from dynamic analyses using the 20 earthquake records. It can be observed that in the 4-story structures maximum inter-story drift occurred in the first story, whereas in the 12-story structures large drift occurred in the higher stories due to the contribution of the higher modes. No discernable difference could be observed between the responses of the building frame system and the dual system. For most earthquake records the maximum inter-story drifts were less than the collapse prevention limit state of 2.5% of the story height (9 cm). Fig. 22 depicts the maximum story displacements obtained from the time-history analysis. Compared with the inter-story drifts, the maximum story displacements in the building frame systems are larger than those in the dual systems.

Fig. 23 presents the location and magnitude of the plastic hinges formed in the 8-story model structures subjected to the El Centro earthquake with peak ground acceleration of 0.35g. It can be
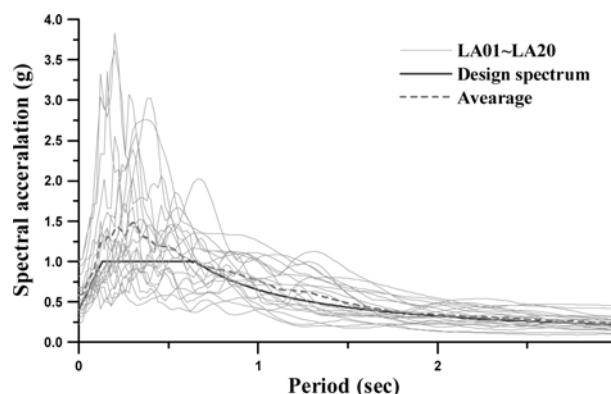

Fig. 20 Response spectra of the 20-earthquake records and the design spectrum
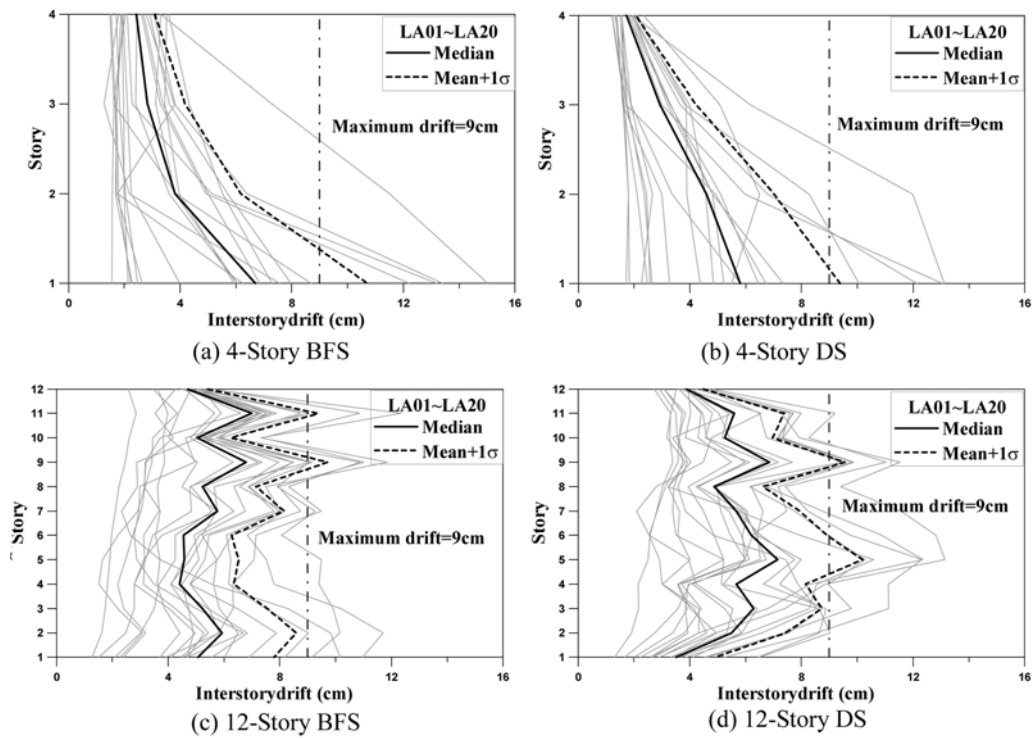
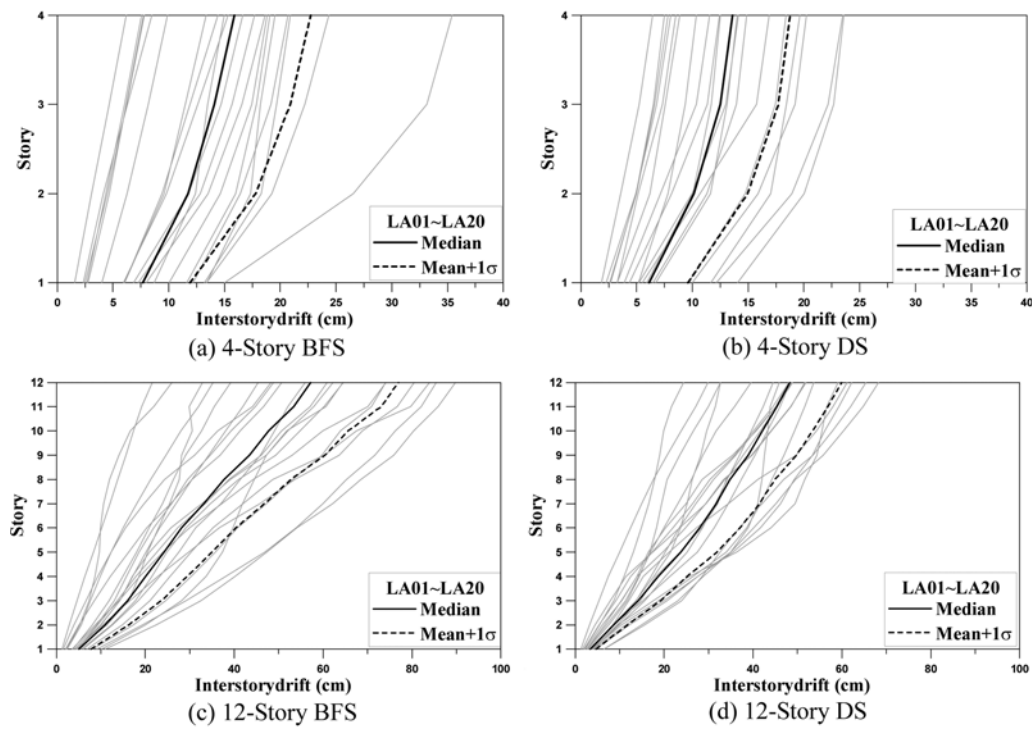Fig. 21 Maximum inter-story drift obtained from time-history analysis

Fig. 22 Maximum story drifts obtained from time-history analysis with 20 earthquake records
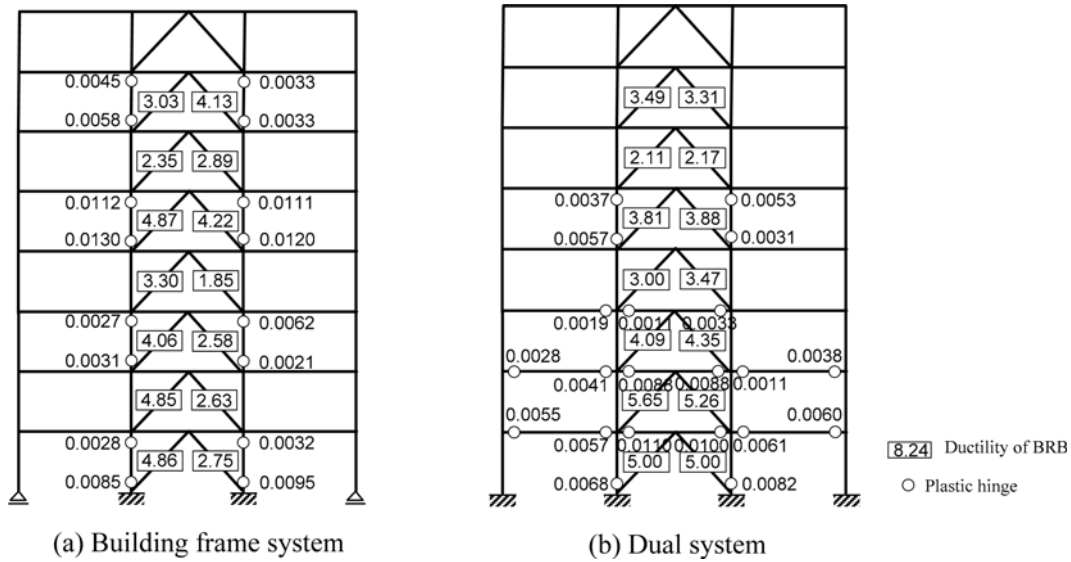
Fig. 23 Maximum plastic hinge rotation and brace ductility ratio of the 8-story structure obtained from time-history analysis using the El Centro earthquake
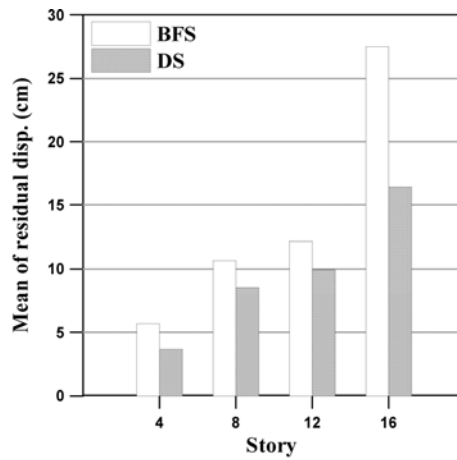

Fig. 24 Maximum residual displacements at the end of dynamic analysis with El Centro earthquake

noticed that the maximum ductility demands in BRB are 4.97 and 5.65 for the building frame systems and the dual systems, respectively, which are less than the collapse prevention limit state recommended in FEMA-450 for braces subjected to tensile load. Also the plastic hinge rotations fall well below the limit state. Fig. 24 shows the top-story residual displacements of the model structures subjected to the El Centro earthquake, where it can be observed that the residual displacements of the dual systems are significantly smaller than those of the building frame systems due to the re-centering capability of the rigid frames. Fig. 25 shows the hysteretic energy time histories of the 4- and 12-story model structures, which show that larger energy is dissipated in the dual systems during the dynamic excitation.
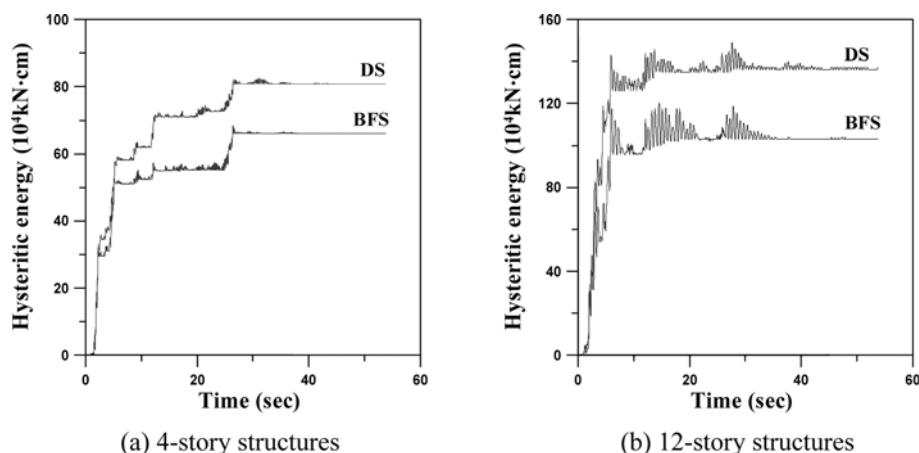
(a) 4-story structures   (b) 12-story structures

Fig. 25 Time history of the hysteretic energy in the model structures subjected to El Centro earthquake

6. Conclusions

In this study the seismic behavior of chevron-type buckling restrained braced frames (BRBF) was investigated and their behavior factors were evaluated. Nonlinear static pushover analyses were carried out to identify the load and the displacement relationship up to the ultimate state. Time history analyses were also carried out to observe dynamic behaviors and to compute the permanent displacement and the dissipated hysteretic energy. The analysis results are summarized as follows:

(1) The behavior factors of BRBFs computed from nonlinear static pushover analyses generally decreased as the number of stories increased. The overstrength factors turned out to be larger than those given in the AISC Seismic Provision; the response modification factors of model structures taller than 4-stories, however, were smaller than those proposed in the provision.

(2) The computed overstrength factors of the dual systems, which were designed with larger response modification factor, were smaller than those of the building frame systems, whereas the ductility factors and the response modification factors of dual systems turned out to be larger than those of the building frame systems. The computed response modification factors decreased as the number of stories increased. The computed response modification factors were not very sensitive to the variation of the design response modification factors. At least based on the limited analysis results of this study, the current response modification factors specified in the design code were generally overestimated, especially in the mid- to high-rise structures.

(3) The maximum inter-story drifts obtained from the time-history analysis with 20 earthquake records were generally less than the collapse prevention limit state of 2.5% of the story height. The hysteretic energy dissipated through plastic deformation in dual systems subjected to the El Centro earthquake was larger than that in building frame system. This resulted in smaller story drift in dual system. Also the residual deformation in dual system was much smaller than in building frame system due mainly to the restoring force provided by the rigid frame.

Acknowledgements

References

AISC (1998), *Load and Resistance Factor Design Specification for Structural Steel Buildings*, American Institute of Steel Construction, Chicago.

AISC/SEAOC (2001), Recommended Provision for Buckling-Restrained Braced Frames (draft).

AISC (2005), *Seismic Provisions for Structural Steel Buildings*, American Institute of Steel Construction, Chicago, Illinois.

ATC (1995), *A Critical Review of Current Approaches to Earthquake-resistant Design*, ATC-34, Applied Technology Council, Redwood City, California, 31-6.

ATC (1995), *Structural Response Modification Factors*, ATC-19, Applied Technology Council, Redwood City, California, 5-32.

Balendra, T. and Huang, X. (2003), "Overstrength and ductility factors for steel frames designed according to BS 5950", *J. Struct. Eng.*, ASCE, **129**(8), 1019-1035.

Black, C., Makris, N. and Aiken, I. (2002), *Component Testing, Stability Analysis and Characterization of Buckling Restrained Unbonded Braces*, Report No. PEER-2002/08, PEERC, University of California at Berkeley.

BSSC (2004), *Recommended Provisions for Seismic Regulations for New Buildings and Other Structures; Part 1: Provisions (FEMA-450)*, Building Seismic Safety Council, Washington, D.C.

BSSC (2000), *Prestandard and Commentary for the Seismic Rehabilitation of Building, FEMA-356*, Federal Emergency Management Agency, Washington, D.C.

BSSC (2001), *Recommended Provisions for Seismic Regulations for New Buildings and Other Structures; Part 2: Commentary.* FEMA-369, Building Seismic Safety Council, Washington, D.C.

Carden, L.P., Itani, A.M. and Buckle, I.G. (2006), "Seismic performance of steel girder bridges with ductile cross frames using buckling-restrained braces", *J. Struct. Eng.*, **132**(3), 338-345.

Choi, H. and Kim, J. (2009), "Evaluation of seismic energy demand and its application on design of buckling-restrained braced frames", *Struct. Eng. Mech.*, **31**(1), 93-112.

Iwata, M. and Murai, M. (2006), "Buckling-restrained brace using steel mortar planks; performance evaluation as a hysteretic damper", *Earthq. Eng. Struct. Dyn.*, **35**, 1807-1826.

ICC (2003), *International Building Code*, International Code Council, Inc., Birmingham, AL.

Kim, J., Choi, H. and Chung, L. (2004), "Energy-based seismic design of structures with buckling-restrained braces", *Steel Compos. Struct.*, **4**(6), 437-452.

Kim, J. and Choi, H. (2005), "Response modification factors of chevron-braced frames", *Eng. Struct.*, **27**(2), 285-300.

Maheri, M.R. and Akbari, R. (2003), "Seismic behavior factor, R, for steel X-braced and knee-braced RC buildings", *Eng. Struct.*, **25**(15), 1505-1513.

Merritt, S., Uang, C.M. and Benzoni, G. (2003), *Subassemblage Testing of Corebrace Buckling-restrained Braces,* Report No. TR-2003/01, U.C. San Diego.

Newmark, N.M. and Hall, W.J. (1982), *Earthquake Spectra and Design,* EERI Monograph Series, Oakland (CA), Earthquake Engineering Research Institute.

Osteraas, J.D. (1990), *Strength and Ductility Considerations in Seismic Design*, Ph.D. dissertation, Stanford University, Stanford, California.

Prakash, V., Powell, G.H. and Campbell, S. (1993), *DRAIN-2DX, Static and Dynamic Analysis of Plane Structure.* NISEE, EERC, U.C. Berkeley.

Somerville, P., Smith, H., Puriyamurthala, S. and Sun, J. (1997), *Development of Ground Motion Time Histories for Phase 2 of the FEMA/SAC Steel Project*, SAC/BD 97/04, Sacramento, CA.

Tremblay, R., Bolduc, P., Neville, R. and DeVall, R. (2006), "Seismic testing and performance of bucklingrestrained bracing systems", *Can. J. Civil Eng.*, **33**, 183-198.

Usami, T., Lu, Z. and Ge, H. (2005), "A seismic upgrading method for steel arch bridges using buckling-restrained braces", *Earthq. Eng. Struct. Dyn.*, **34**, 471-496.

Valles, R.E., Reinhorn, A.M., Kunnath, S.K., Li, C. and Madan, A. (1996), *IDARC 2D version 4.0: A Computer Program for the Inelastic Damage Analysis of Buildings*, Technical Report NCEER-96-0010, National Center for Earthquake Engineering Research, State University of New York at Buffalo.

Vamvatsikos, D. and Cornell, C.A. (2001), "Incremental dynamic analysis", *Earthq. Eng. Struct. Dyn.*, **31**(3), 491-514.

Xie, Q. (2005), "State of the art of buckling-restrained braces in Asia", *J. Constr. Steel Res.*, **61**, 727-748.